Transient Behavior of Pulsed Particulate Fluidized Beds

L. A. M. van der Wielen, A. W. K. G. Sjauw Koen Fa, J. J. M. Potters, and K. Ch. A. M. Luyben
Dept. of Biochemical Engineering, Delft University of Technology, Julianalaan 67 2628 BC Delft, The Netherlands

Transient phenomena in solid–liquid fluidized-bed systems are important in designing pulsed, countercurrent (multistage) fluidized-bed contactors of the Cloete-Streat type at high-solids flow rate. Of particular interest are the residence times or corresponding velocities of porosity gradients in the bed and the excess or overshoot height of the bed after refluidization. Theory assuming local equilibrium between holdup and velocity of the phases (local-equilibrium model) for stepwise perturbations in the liquid flow is readily available. It is investigated whether the local-equilibrium theory can be used for more complex perturbations and whether inertia effects, such as are encountered in countercurrent multistage fluidized-bed systems, can be ignored. Therefore, the detailed particle-bed model of Foscolo and Gibilaro, which incorporates inertia effects, was applied to investigate the transient behavior of fluidized-bed systems. Transient fluidization experiments were performed with a broad range of water-fluidized particles in a laboratory-scale multistage fluidized-bed contactor. The operating conditions corresponded to those for countercurrent contact.

Numerical simulations with the particle-bed model predict satisfactory experimental results. The "overshoot" heights of the fluidized bed were estimated correctly by the particle-bed model, whereas the local-equilibrium model only provides a conservative estimate. However, the local-equilibrium model allows an analytical solution that is more interesting for design, as it avoids tedious calculations. The residence time of the last perturbation before the fluidized bed relaxes to steady state was estimated with similar accuracy by both models.

Introduction

Pulsed multistage fluidized-bed contactors employ periodic flow reversal and refluidization to establish semicontinuous countercurrent solids transport (Streat, 1980). Depending on the frequency and magnitude of the flow-reversal and refluidization cycles, transient phenomena may play an important role in determining both the maximum flow rate and effective holdup of the solids. Applications of pulsed multistage liquid fluidized-bed contactors have been described for continuous ion exchange (Streat, 1980), continuous adsorption of biomolecules (Van der Wiel and Wesselingh, 1988), and as continuous reactor for deactivating biocatalysts (Vos, 1990). Recently, the application of this concept as countercurrent adsorptive reactor, in which selective countercurrent transport of dense adsorbent particles was combined with the retention of a lighter biocatalyst phase, was proposed (van der Wielen et al., 1990).

In transient pulsed fluidized-bed systems such as the multistage Cloete-Streat contactors, complex fluctuations in the liquid velocity are found. Reliable predictions of the transient behavior of pulsed fluidized beds aimed at equipment design require accurate and yet the simplest possible mathematical description. Transient behavior of particulate fluidized beds was studied as early as 1959 by Slis and coworkers (1959). They investigated the response of a liquid fluidized bed to stepwise changes in the liquid velocity. Fan et al. (1963) extended the observations for glass-bead–water systems subject to pulse and sinoidal disturbances. Didwania and Homsy (1981) performed stepwise expansion experiments in low porosity ($\epsilon = 0.38$–0.58) glass-bead–water flu-

Correspondence concerning this article should be addressed to L. A. M. van der Wielen.

idized beds. In all cases, a rich dynamic behavior was observed.

Slis et al. (1959) provided a mechanistic description of both collapse and expansion behavior, to support their ideas. The essential assumption in their model is local equilibrium of bed porosity, liquid, and particle velocity, according to the Richardson and Zaki relation (1954). This approach neglects the effects of inertia. We refer to this model as the local-equilibrium model. Fan and coworkers (1963) derived a linearized model of the (nonlinear) local-equilibrium model of Slis et al. (1959). In the linearized model, time constants were estimated from the reference system properties. Although deviations from the reference state were encountered experimentally, they found fairly accurate predictions of step, pulse, and sinus responses.

The flow history of a pulsation cycle in a multistage fluidized bed (fluidization, abrupt flow reversal, and refluidization) is less smooth. The assumption of negligible inertia effects may not be generally valid in these systems (Wallis, 1969). Therefore, it is not clear whether the dynamic behavior is adequately described with the (reduced) local-equilibrium model, or if a more detailed approach is required. A more detailed approach is the particle-bed model of Foscolo and Gibilaro (1987), which takes the unsteady momentum balance into account.

Aim of this work

In this article, calculations with the local-equilibrium model are compared to those from the particle-bed model of Foscolo and Gibilaro (1987). Both models consist of single or multiple nonlinear, coupled hyperbolic partial differential equations that have to be solved numerically. An implicit finite difference method for hyperbolic conservative-law equations as derived by Wilders (1985) is adopted for this purpose. The computational results of both models are compared to experimental data obtained in a laboratory-scale multistage fluidized bed. Some approximate design criteria for the pulsed multistage fluidized-bed contactors, have been derived that allow for estimation of the transient effects.

Theory

Particle-bed model

Starting from a complete set of mass and momentum balances for both phases, Foscolo and Gibilaro (1987) obtained a reduced self-contained formulation of the equations of change for a fluidized bed, consisting of the differential continuity and momentum balances for the particle phase only. The one-dimensional continuity and momentum conservation equations for the particle phase read

$$\frac{\partial(1-\epsilon)}{\partial t}+\frac{\partial}{\partial z}[(1-\epsilon)u_p]=0 \tag{1}$$

and

$$(1-\epsilon)\rho_p\left[\frac{\partial u_p}{\partial t}+u_p\frac{\partial u_p}{\partial z}\right]-u_E^2\rho_p\frac{\partial \epsilon}{\partial z}=\mathfrak{F}. \tag{2}$$

The net force on the particles, $\mathfrak{F}$, consists of buoyancy, gravity, and the averaged, volumetric interaction of a particle with the fluidized bed and equals

$$\mathfrak{F}=(\rho_p-\rho_L)g\left(\left(\frac{u_o-u_p}{u_t}\right)^{4.8/n}\epsilon^{-4.8}-1\right)\epsilon(1-\epsilon). \tag{3}$$

The "elastic wave velocity" u_E (Foscolo and Gibilaro, 1987) in Eq. 2 is the velocity of a longitudinal pressure wave through the particulate bed and is given by

$$u_E=\left[3.2gd_p(1-\epsilon)\left(\frac{\rho_p-\rho_L}{\rho_p}\right)\right]^{0.5}. \tag{4}$$

The set of differential Eqs. 1–4 forms an initial-value problem. Hence, only boundary conditions at the bed entrance and the initial porosity and velocity distribution are required. We have assumed that the local porosity at the bed entrance corresponds instantaneously to the actual superficial velocity according to the Richardson and Zaki relation (1954). Furthermore, zero slip for the particles is assumed at the bed entrance. The initial conditions are uniform steady-state porosity throughout the fluidized bed and zero particle velocity.

$$\epsilon(x=0,t)=\epsilon_0(t); \qquad u_p(x=0,t)=0. \tag{5}$$

The numerical solution by the finite difference technique of Wilders (1985) requires that the set of Eqs. 1–4 is rewritten as a set of general conservation-law equations:

$$\frac{\partial w}{\partial t}+\frac{\partial F(w)}{\partial z}=s(w). \tag{6}$$

The quantity F is the conserved flux. The conserved variables and fluxes of the particle-bed model are given by the following expressions:

$$w=\begin{pmatrix}\epsilon\\ u_p\end{pmatrix} \quad \text{and} \quad F=\begin{pmatrix}-(1-\epsilon)u_p\\ \frac{u_p^2}{2}-3.2gd_p\left(\frac{\rho_p-\rho_L}{\rho_p}\right)\epsilon\end{pmatrix}. \tag{7}$$

The source term s is given by

$$s=\begin{pmatrix}0\\ g\epsilon\left(\frac{\rho_p-\rho_L}{\rho_p}\right)\left(\left(\frac{u_0-u_p}{u_t}\right)^{4.8/n}\epsilon^{-4.8}-1\right)\end{pmatrix} \tag{8}$$

Local-equilibrium model

The local equilibrium model (Slis et al., 1959) is obtained analogously by replacing u_p by the algebraic equilibrium relation of Richardson and Zaki (1954):

$$u_L-u_p=u_t\epsilon^{n-1}. \tag{9}$$

Substitution in Eq. 1 gives the single equation of the equilibrium model:

$$\frac{\partial \epsilon}{\partial t} + \frac{\partial}{\partial z}[-(1-\epsilon)(u_{Lo} - u_t \epsilon^{n-1})] = 0. \qquad (10)$$

This equation is already in conservation form and ready for computation. Initial and boundary conditions are similar to those of the particle-bed model.

Numerical solution of the models and the use of marker particles

Both models were solved numerically by the method described by Wilders (1985). The position of the bed end varies with time and cannot coincide with the end of a spatially fixed computational domain. Therefore the computational domain is taken to be larger than the maximum bed length. The trajectory of the physical-bed end is tracked by following the position of a so-called "marker particle" (Kuipers, 1990). This marker particle is located initially at the bed end. By numerical integration in time of the velocity of this marker particle, the time-dependent location z_m can be computed according to Eq. 11:

$$z_m(t) = z_m(t=0) + \int_0^t u_p(z_m) d\tau. \qquad (11)$$

These "particles" do not interfere with the actual computation. They can be added to both the solid and liquid phase to study the trajectories of selected portions of the bed.

Experimental Studies

Multistage fluidized-bed system

The transient behavior of various water-fluidized particles has been studied in a laboratory-scale fluidized-bed contactor of the Cloete-Streat type, which was described earlier (van der Wielen et al., 1990). The experimental setup consists of a perspex contactor 0.75 m long and 40.3 mm internal diameter. The contactor has two sections to facilitate the mounting of sieve plates. The system is equipped with a pulseless rotary gear pump, a magnetoinductive flowmeter, and a pulsation system as described by Vos et al. (1990). The pulsation tube had a volume of 16 mL and contained a polypropylene float that was used to activate the two optical sensors determining the pulsation volume. The frequency of the pulsation was set at 0.05 Hz (3 min^{-1}) unless indicated otherwise. Under these conditions, the individual waves and bed-height responses could be distinguished. When the pulsation frequency was increased to 0.1 Hz or higher, the interaction of subsequent responses was observed. A complete pulsation cycle consists of the flow reversal in the column by opening a recycle over the rotary gear pump and by taking a specified amount of liquid out of the system. In this case, the amount of liquid taken was 16 mL. The movement of the float took, depending on the system, 1–1.4 s. This resulted in the forced transport of the fluidized-bed contents toward the bottom sieve plate, resulting in a bed of particles at the sieve plate. A part of the bed material was removed through the sieve plate and the same amount was added from the upper sieve plate during this flow-reversal period. Various checks indicated that the particle content of the compartment remained constant. Then the float was pushed back to its original position by means of compressed air in about 1 s. Simultaneously, the recycle over the rotary gear pump was closed, allowing refluidization to start. As the bed in the former period was not in a fluidized state, its behavior during that period could not be described in this work using any model. Therefore, we have focused on the refluidization period only, taking the measured overall flow rate from gear pump and pulsation tube as input data for the numerical code.

The following modifications were made to the experimental setup described earlier. Only two sieve plates with a conical bore were mounted. The flow rate was monitored on-line via the magnetoinductive flowmeter using an HP Vectra ES/12PC. The behavior of the fluidized bed was registered with a Panasonic VHS video camera. The time code and the number of video frames per second allowed a 0.04 s accuracy in the determination of the time. The resolution of the frames allowed a determination of the bed-end position with an accuracy of 1–2 mm. The propagation of porosity waves could be observed clearly in the "movie picture" from its texture, but the exact location could not be determined from the individual frames, as the contrast was too low. Instead, the transient bed height vs. time was measured from a frame-by-frame playback of the videotape.

Particles

Particles with a broad range of densities and sizes were used in the experiments. Table 1 summarizes the particle properties and the experimental conditions used. Densities were determined by the repeated addition of particles to a calibrated, water-filled cylinder, while simultaneously recording the added volume and mass. The densities were deter-

Table 1. Properties of the Particles and Experimental Conditions Used in this Work

Code	Composition	Dia. mm	Density kg/m^3	u_t cm/s	n	u_{Lo} cm/s
I	Maxazyme	1.27	1,100	2.92	3.24 ± 0.10	0.39,0.58,0.75,0.95
II	Zeolite pellet	1.74	1,175	7.35	3.88 ± 0.13	0.39,0.58,0.77,0.95,1.12
III	Cu-alginate	1.46	1,280	7.76	3.19 ± 0.07	0.45,0.83,1.18,1.54
IVa	Glass	0.77	2,560	18.64	3.90 ± 0.07	1.01,1.29,1.64,2.00
IVb	Glass	1.31	2,560	29.45	3.57 ± 0.03	1.13,1.31,1.73,2.13
Va	Glass	0.34	2,875	7.82	3.48 ± 0.03	0.81,1.17,1.55,2.00
Vb	Glass	0.44	2,875	10.02	3.40 ± 0.07	0.95,1.28,1.63,2.04
Vc	Glass	0.66	2,875	14.44	3.73 ± 0.10	0.98,1.35,1.73,2.10
Vd	Glass	0.98	2,875	18.90	3.59 ± 0.04	1.16,1.50

mined within 0.5% error. The particle-size distribution of all particles was determined using a Joyce-Loebl Magiscan 2A image analyzer. The particle-size distribution was ± 100 μm, except for particle types III, Va, and Vb (± 200 μm). A segregation tendency was only observed for the very small glass beads Va and Vb. All particle types were spherical. The terminal velocity and the Richardson and Zaki exponent n were determined from steady-state fluidization experiments at various flow rates in the fluidized-bed system described earlier.

Results

Experimental vs. simulated pulsation cycles

Characteristic experimental results, giving the bed heights vs. time are shown in Figure 1 for particles with relatively low density (type II). The particle-bed model predictions are also shown in Figure 1. In this figure, a characteristic "overshoot" is observed. This is caused by the pushback of the liquid from the pulsation tube into the fluid bed. The pushback resulted in a high voidage "plug" propagating through the fluidized bed. The top of the overshoot corresponds with the time at which the front of the plug reaches the bed end. Then the particles move downward because of the high porosity in the plug, and the bed relaxes to its steady-state height. Similar experiments have been performed for all velocities indicated in Table 1, and simulations have been performed for each of them. In general, good agreement between the experimental results and the predictions by the particle-bed model was observed.

Time constants for particle acceleration were obtained by Gibilaro et al. (1984), and are one or two orders of magnitude smaller than those for the motion of continuity waves or for the complete expansion–contraction process. For step responses, the particle velocity is virtually in equilibrium with the local particle hold-up in the system. However, for the systems with complex flow-rate patterns that lead to multiple accelerations and decelerations, the particle-bed model is likely to give different results than the local-equilibrium model.

Comparison of the calculations of the transient behavior of a fluidized bed of low-density, type II particles, as is shown in Figure 1, supports this statement. Incorporation of added mass in the equations (Gibilaro et al., 1984) appeared unnecessary, as its effect on the propagation of continuity waves of relatively light particles seems to be negligible.

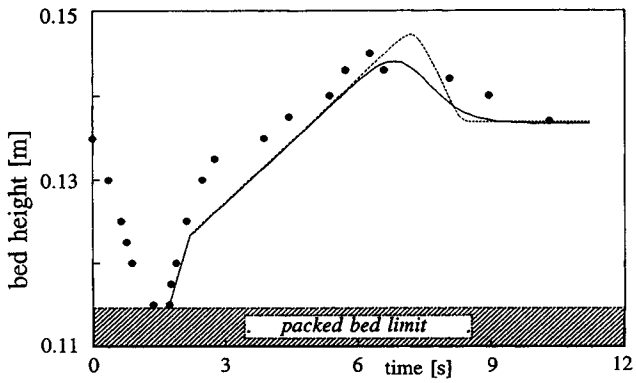

Figure 1. Particle-bed (solid curve) vs. local-equilibrium models (dotted curve).

Data (markers): particle II (Table 1, run 3); steady-state velocity is 7.7 mm/s

Experimental transient bed heights are shown as solid spheres in Figure 1. Both models give a fair, although not identical description of the actual experimental behavior. This was also observed for the other experiments. The overshoot height appears to be slightly better estimated by the particle-bed model. Hence, the general conclusion from this comparison is that the assumption of local equilibrium of particle velocity and bed porosity is not always justified.

However, the local-equilibrium model consists of only one partial differential equation instead of two for the particle-bed model. By applying the local-equilibrium model, the smallest time constant is removed from the set of equations. The time step in the local-equilibrium model is determined by the propagation of continuity waves and therefore can be larger than for the particle-bed model. The overall effect is a tenfold reduction of CPU time with a limited loss of accuracy.

Design criteria for pulsed (multistage) fluidized contactors

For an optimal design of pulsed multistage fluidized-bed contactors, the magnitude of the dynamic phenomena related to the cyclic flow-reversal–refluidization operation should be estimated. Two dynamic phenomena of relevance are the overshoot due to the liquid backpush, and the relaxation time t_R, after which all continuity shock waves introduced by the pulse have left the fluidized bed. The occurrence of the *overshoot* phenomenon in pulsed fluidized beds necessitates a larger compartment size then in the case of steady-state fluidization. The extent of overshoot, depends, of course, on particle properties and the manner of pulsation. In some cases, we observed an overshoot as high as 25% of the steady-state bed length. In an earlier section it was indicated that the particle-bed model provides in most cases an acceptable description of the overshoot amplitude. This is summarized in Figure 2, which is a parity plot of the overshoot amplitudes of experimental and simulated refluidizations for series II, III, IVa and IVb. Similar results (not shown) have been obtained for the relaxation time t_R.

Overshoot Amplitude. The particle-bed model is not very convenient for design purposes because it requires a numerical solution. We will derive analytical criteria for the estimation of the amplitude of the overshoot of the pulsation and for the time required for relaxation of the fluidized bed t_R. First, we consider the propagation of the high voidage plug wave resulting from the refluidization. Figure 3 presents the transient expansion–contraction behavior of a fluidized bed of type II particles. The various shaded regions correspond to portions and time intervals of the fluidized bed with the original steady-state porosity (I), the packed state caused by the flow reversal (II), and the high voidage plug (III). The continuity wave (II $\rightarrow$ III) gives the time t^* and amplitude H^* of the overshoot. The continuity wave (III $\rightarrow$ I) gives the time required by the bed to relax to the steady state, t_R. The propagation velocities can be readily computed from the work of Slis et al. (1959).

The maximum pulsation frequency is limited by the relatively slow propagation of continuity waves. Here, we con-

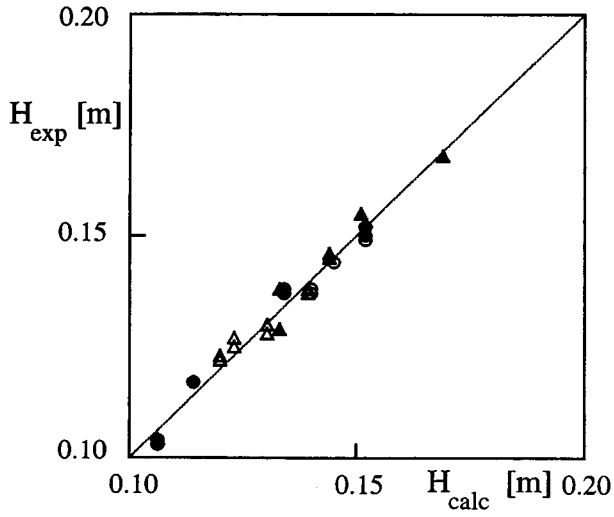

Figure 2. Parity of refluidization "overshoot" amplitudes of experiment and numerical simulations with the particle-bed model.

Particles: II(▲), III(●), IVa(△), IVb(○), according to Table 1.

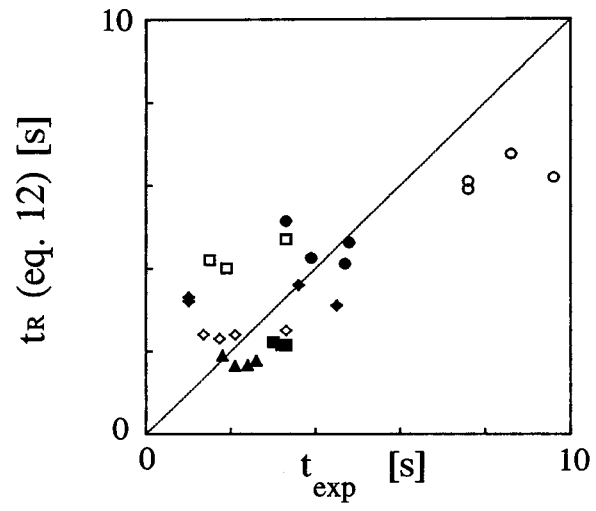

Figure 4. Parity of experimental relaxation times t_R and those computed with Eq. 12.

Particles: I(Δ), II(○), III(●), IVa(▲), IVb(■), Va(□), Vb(♦), and Vc(◇), according to Table 1.

sider the propagation velocity of the continuity wave resulting from the end of the pulsation cycle. This wave is shown in Figure 3 as the (III → I)-transition. The velocity of this wave and the steady-state bed height determine the minimal relaxation time of the bed t_R and thus the maximum pulsation frequency. The wave velocity can be estimated from the magnitude of the superficial flow rate during the pushback of the float and in the final situation, using the work of Slis et al. (1959):

$$t_R = (t_2 =) \frac{\epsilon_2 H_2}{nu_{Lo,2}(1-\epsilon_2)}. \qquad (12)$$

As the steady-state bed height H_2 and porosity ϵ_2 at the final conditions (indicated with subscript 2) are known, the sum of the residence time of this wave in the bed and the actual time interval of liquid reversal (t_C) gives the complete relaxation time. Figure 4 is a parity plot of experimental relaxation times (without t_C) and those predicted using Eq. 12.

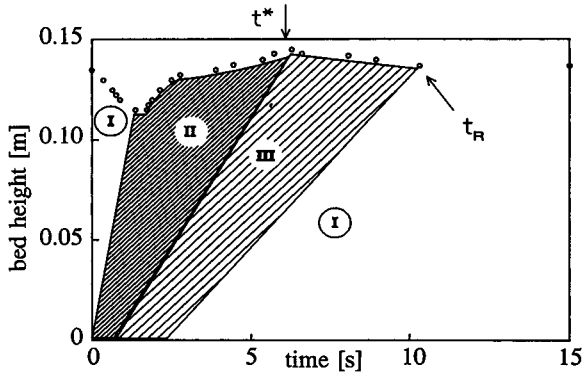

Figure 3. Pulsation cycle in a fluidized bed of type II particles at 0.77 cm/s.

Regions: steady-state bed (I), packed bed (II), and high-voidage plug (III). Points are experimental bed heights.

Estimation of the Overshoot Amplitude from the Local-Equilibrium Model. Figure 3 indicates that at the time of the maximum overshoot, the fluidized bed might consist of two zones with a different porosity: zone III and Zone I. The ratio of the upper high voidage plug (III) and the lower porosity steady-state bed zone (I) can be computed from the overall solids balance and the propagation velocities of the (II → III) and (III → I)-interfaces through the bed. We assume that the wave associated with the (II → III)-interface corresponds to the stepwise transition of a fixed bed to a corresponding bed with a superficial velocity equal to the overall flow rate at the start of the refluidization (gear pump and pulsation tube). A similar assumption is made for the (III → I)-interface. The velocities of both interfaces can then be computed from the expression for the propagation velocity of a continuity shock wave, as demonstrated by Wallis (1969). The bed height and the time at which the bed reaches its maximum, H^* and t^*, respectively, can be calculated from these velocities and an overall mass balance for the fluidized bed. Figure 5 gives the parity plot of the overshoot amplitudes that are calculated in this way and the corresponding experimental values. The calculated overshoot amplitudes overestimate the true amplitudes. This is expected, as the local-equilibrium model does not account for inertia effects, as is clearly shown in Figure 1. Hence, this procedure provides a conservative criterion for the extent of the overshoot.

Conclusions

The transient behavior of particulate fluidized beds can be computed from any of the models presented in this work. Because of the relative ease of calculation, the local-equilibrium model is preferred when the description of wave propagation, bed expansion, and contraction are considered. When inertia effects, such as repetitive acceleration–deceleration phenomena, are to be considered, the particle-bed

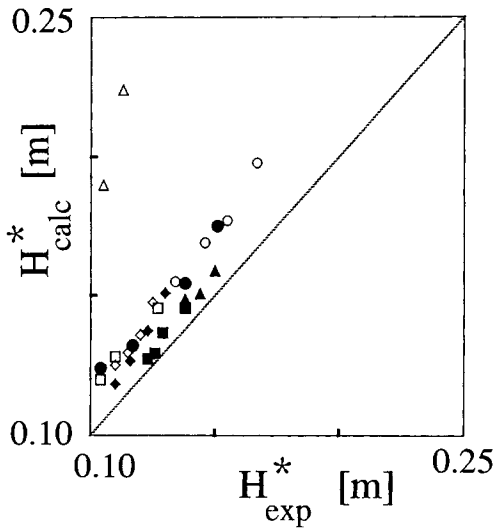

Figure 5. Parity of experimental "overshoot" amplitudes H^* and those computed from the simplified version of the local-equilibrium model.

Particles: I(Δ), II(○), III(●), IVa(▲), IVb(■), Va(□), Vb(◆), and Vc(◇), according to Table 1.

model should be applied. The numerical solution of both models could be efficiently calculated with the compact finite difference method of Wilders, giving stable solutions for severe input conditions.

Model predictions and experimental data from a pulsed-liquid fluidized contactor match well over a broad range of particle and fluidization characteristics. With respect to the design of pulsed multistage fluidized-bed systems such as the Cloete-Streate contactor, transient aspects cannot be neglected. First, the observed overshoot caused by the pulsation mechanism might lead to the unwanted axial transport of solid material to the upper stages. Second, the period that the fluidized bed requires for regaining its steady-state height largely exceeds the actual time of the pulsation. In this study of relatively small beds of 10–15 cm, the ratio of relaxation time and pulsation time is 3–4, but this ratio increases with increased bed length. This restricts the maximum pulsation frequency and thus the maximum solids transport.

Acknowledgments

Part of this work was supported financially by the Netherlands Organization for Scientific Research (N.W.O.). Gist-brocades N.V. is acknowledged for the free gift of Maxazyme particles. Dr. P. Wilders of the Department of Applied Mathematics is gratefully acknowledged for providing the numerical algorithm and for his assistance in the implementation.

Notation

d = particle diameter, m
g = gravity constant, $m^2 \cdot s^{-1}$
u = linear velocity, $m \cdot s^{-1}$
u_ϵ = continuity wave velocity, $m \cdot s^{-1}$
u_0 = approach velocity, $m \cdot s^{-1}$
z = axial coordinate, m
ρ = density, $kg \cdot m^{-3}$

Subscripts

L = liquid phase
0 = equilibrium conditions
s = slip conditions

Literature Cited

Didwania, A. K., and G. M. Homsy, "Rayleigh-Taylor Instabilities in Fluidized Beds," *Ind. Eng. Chem. Fundam.*, **20**, 318 (1981).

Fan, L.-T., J. A. Schmitz, and E. N. Miller, "Dynamics of Liquid-Solid Fluidized Bed Expansion," *AIChE J.*, **9**(2), 149 (1963).

Foscolo, P. U., and L. G. Gibilaro, "Fluid Dynamic Stability of Fluidized Suspensions: The Particle Bed Model," *Chem. Eng. Sci.*, **42**(6), 1489 (1987).

Gibilaro, L. G., S. P. Waldram, and P. U Foscolo, "A Simple Mechanistic Description of the Unsteady State Expansion of Liquid Fluidized Beds," *Chem. Eng. Sci.*, **39**(3), 607 (1984).

Gibilaro, L. G., R. di Felice, and P. U. Foscolo, "Added Mass Effects in Fluidized Beds: Application of the Geurst-Wallis Analysis of Inertial Coupling in Two Phase Flow," *Chem. Eng. Sci.*, **45**(6), 1561 (1990).

Kuipers, J. A. M. "A Two-fluid Micro Balance Model of Fluidized Beds," PhD Thesis, University of Twente, Quick Service Drukkerij, Enschede, The Netherlands (1990).

Richardson, J. F., and W. N. Zaki, "Sedimentation and Fluidization: I," *Trans. Inst. Chem. Eng.*, **32**, 35 (1954).

Slis, P. L., Th. W. Willemse, and H. Kramers, "The Response of the Level of a Liquid Fluidized Bed to a Sudden Change in the Fluidizing Velocity," *Appl. Sci. Res.*, **A8**, 209 (1959).

Streat, M., "Recent Developments in Continuous Ion Exchange," *J. Sep. Proc. Technol.*, **1**(3), 10 (1980).

van der Wiel, J., and J. A. Wesselingh, "Continuous Adsorption Biotechnology," *Adsorption: Science and Technology*, A. E. Rodrigues, M. D. LeVan, and D. Tondeur, eds., NATO-ASI Series Vol. 158, 427 (1988).

van der Wielen, L. A. M., A. J. J. Straathof, J. J. M. Potters, and K. Ch. A. M. Luyben, "Integration of Bioconversion and Chromatographic Product Separation by Means of Countercurrent Adsorption," *Chem. Eng. Sci.*, **45**(8), 2397 (1990).

Vos, H. J., M. Zomerdijk, D. J. Groen, and K. Ch. A. M. Luyben, "Countercurrent Multistage Fluidized Bed Reactor for Immobilized Biocatalysts: II. Operation of a Laboratory Scale Reactor," *Biotechnol. Bioeng.*, **36**, 377 (1990).

Wallis, G. B., *One-Dimensional Two-Phase Flow*, McGraw-Hill, New York (1969).

Wilders, P., "An Unconditionally Stable Implicit Method for Hyperbolic Conservation Laws," *J. Eng. Math.*, **19**, 33 (1985).

Manuscript received Dec. 5, 1995, and revision received Sept. 26, 1996.